Biosci. Biotechnol. Biochem., **76** (3), 559–566, 2012

Molecular and Catalytic Properties of Monoacetylphloroglucinol Acetyltransferase from *Pseudomonas* sp. YGJ3

Asuka HAYASHI,[1] Hiroki SAITOU,[1] Tomomi MORI,[1] Ikue MATANO,[1] Hiroyuki SUGISAKI,[2] and Kiyofumi MARUYAMA[1,†]

[1]*Department of Biomolecular Science, Faculty of Engineering, Gifu University, 1-1 Yanagido, Gifu 501-1193, Japan*
[2]*Institute for Chemical Research, Kyoto University, Uji, Kyoto 611-0011, Japan*

Received November 10, 2011; Accepted December 20, 2011; Online Publication, March 7, 2012
[doi:10.1271/bbb.110860]

Monoacetylphloroglucinol (MAPG) acetyltransferase, catalyzing the conversion of MAPG to 2,4-diacetylphloroglucinol (DAPG), was purified from *Pseudomonas* sp. YGJ3 grown without Cl^-. Cl^- and pyoluteorin repressed expression of the enzyme. SDS-polyacrylamide gel electrophoresis showed that the purified enzyme (M_r = 330 kDa) was composed of three subunits of 17, 38, and 43 kDa, and protein sequencing identified these as PhlB, PhlA, and PhlC respectively. The enzyme catalyzed the reversible disproportionation of 2 moles of MAPG to phloroglucinol (PG) and DAPG. The equilibrium constant K (=[DAPG][PG]/[MAPG]^2) was estimated to be about 1.0 at 25 °C. A *Kpn*I 20-kb DNA fragment was cloned from the genomic DNA of strain YGJ3, and a 12,598-bp long DNA region containing the *phl* gene cluster *phlACBDEFGHI* was sequenced. PCR cloning and expression of the *phl* genes in *Escherichia coli* confirmed that expression of *phlACB* genes produced MAPG ATase.

Key words: acetyltransferase; diacetylphloroglucinol; disproportionation; monoacetylphloroglucinol; phloroglucinol

Fluorescent pseudomonads produce a variety of secondary metabolites that more or less affect microbial growth in microflora.[1)] Secondary metabolites showing strong antibiotic activity are useful in medical and pharmaceutical applications.[2)] Polyketide 2,4-diacetylphloroglucinol (DAPG), chlorinated pyrrole pyoluteorin, and phenazine-1-carboxylate are particularly important in agriculture due to their potent anti-fungal effects in the rhizosphere.[2–4)] Among these, DAPG has a broad spectrum of antifungal activity, and is a key compound for the biocontrol activity of fluorescent pseudomonads.[5–7)] Bacterial strains with a high capacity for DAPG production effectively suppress the plant diseases caused by pathogenic fungi such as take-all disease, found in wheat, black root rot in tobacco, and the damping-off of sugar-beet seedlings.[8–10)]

To establish a reliable biocontrol with fluorescent pseudomonads, it is essential to understand fully the mechanism and the regulation of DAPG biosynthesis. DAPG is biosynthesized under the direction of *phl* gene cluster *phlACBDEFGHI*.[7,11–14)] Among these, genes *phlEFGH* are not directly involved in the synthetic process of DAPG: PhlE and PhlG are a putative permease and a DAPG hydrolase respectively,[13–15)] and PhlF and PhlH are DAPG synthetic pathway-specific transcriptional regulators.[12,14)] PhlI is a putative uncharacterized protein (UniProt accession no. C0J9E0).[7)] Bangera and Thomashow cloned the *phlACBDEF* genes from *Pseudomonas fluorescens* Q2-87, and found that DAPG biosynthesis depended on the *phlACBD* genes.[11)] Based on qualitative analysis of gene function, they proposed a possible mechanism for DAPG biosynthesis: PhlA, PhlC, and PhlB jointly catalyze acyl transfer both at the initial step, the formation of acetoacetyl-CoA from acetyl-CoA, and at the final step, the acetylation of monoacetylphloroglucinol (MAPG) to DAPG. PhlD which shows a high level of homology to chalcone synthase, a type III-polyketide synthase,[16,17)] is assumed to catalyze the elongation through sequential condensation of malonyl-CoA to acetoacetyl-CoA and the cyclization of the polyketide chain to MAPG. Shanahan *et al.* measured the enzymatic acetylation of MAPG to DAPG by HPLC with a cell-free extract of *Pseudomonas* sp. F113, and named the enzyme MAPG acetyltransferase (ATase).[18)] Although PhlA, PhlC, and PhlB are necessary for MAPG ATase activity, the correct characterization of MAPG ATase molecule remains unknown.

Achkar *et al.* found enzymatic evidence for the formation of a polyketide chain.[19)] They cloned the *phlACBDE* genes from *P. fluorescens* Pf-5 and found that recombinant *Escherichia coli* carrying a plasmid with a *phlD* insert markedly produced phloroglucinol (PG), a condensation product of three molecules of malonyl-CoA. Subsequently, Zha *et al.* prepared a PhlD-His_6 (PhlD whose C-terminus is tagged with His_6), and found that PhlD-His_6 catalyzed the synthesis of PG from malonyl-CoA.[20)] Hence it is expected that MAPG ATase is involved in the sequential acetylation of PG to give MAPG and DAPG. To test this possibility, a homogeneous preparation of MAPG ATase is required.

In a previous study, we isolated the pyoluteorin/DAPG-producing bacterium *Pseudomonas* sp. YGJ3 and found that strain YGJ3 mainly produced pyoluteorin

† To whom correspondence should be addressed. Fax: +81-58-294-4633; E-mail: maruyama@gifu-u.ac.jp

Abbreviations: ATase, acetyltransferase; DAPG, 2,4-diacetylphloroglucinol; IPTG, isopropyl β-thiogalactopyranoside; MAPG, monoacetylphloroglucinol; PAGE, polyacrylamide gel electrophoresis; PG, phloroglucinol

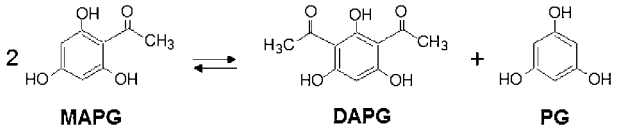

Fig. 1. Acetyl Transfer Catalyzed by MAPG ATase.

during growth in the presence of Cl^-, while it produced DAPG in the absence of Cl^-.[21] Production of DAPG was strongly inhibited by Cl^- or pyoluteorin in the culture medium, whereas Br^- and I^- were almost ineffective. Consistently with this, significant activity of MAPG ATase was observed in cell-free extract prepared from bacterial cells grown without Cl^-. The activity decreased markedly when strain YGJ3 was grown in the presence of Cl^- or pyoluteorin. In the present study, based on these findings, *Pseudomonas* sp. YGJ3 was cultivated in the absence of Cl^- to achieve a high degree of expression of MAPG ATase, and MAPG ATase was purified from an extract of bacterial cells to examine its molecular and catalytic properties. We found for the first time that MAPG ATase is composed of PhlA, PhlC, and PhlB, and that it catalyzes the disproportionation of 2 moles of MAPG to phloroglucinol (PG) and DAPG (Fig. 1). Furthermore, a *phl* gene cluster was cloned from strain YGJ3, confirming that genes *phlACB* encode MAPG ATase.

Materials and Methods

Chemicals. MAPG and DAPG were purchased from Tokyo Chemical Industry (Tokyo) and Toronto Chemical Research (Toronto, Canada) respectively. Pyoluteorin was isolated from culture broth of *Pseudomonas* sp. YGJ3 as described previously.[21] All other chemicals were of commercially available analytical grade.

Microorganisms. Pseudomonas sp. YGJ3 (Faculty of Engineering, Gifu University) was aerobically cultivated at 30 °C for 24 h in a synthetic liquid medium in which Cl^- was excluded and ethanol was used as carbon and energy source, as described previously.[21] Bacterial cells were collected by centrifugation at 4 °C, washed with 50 mM potassium phosphate (pH 7.0), and stored at −25 °C until needed. *E. coli* XL1-Blue MRA as host for Charomid vector and XL1-Blue MRF′ as host for the plasmid vector were from Stratagene (La Jolla, CA).[22] The former was grown at 37 °C in Luria-Bertani (LB) medium (polypeptone 20 g, yeast extract 10 g, and NaCl 20 g per 1 L of distilled H_2O, pH 7.0), and the latter in LB medium containing tetracyclin (10 μg/mL).

Purification of MAPG ATase. Unless otherwise specified, all manipulations were done at 0–4 °C with 50 mM potassium phosphate buffer (pH 7.0). Bacterial cells (20 g, wet weight) were suspended with 60 mL of the buffer and broken with a Sonifier (Branson, Danbury, CT). After centrifugation at 30,000 × *g* for 15 min, the supernatant solution (crude extract) was treated with $(NH_4)_2SO_4$. The precipitate obtained between 35 and 65% saturation was collected by centrifugation and dissolved in about 18 mL of the buffer. Half of the solution was put on a column (3 × 30 cm) of Superdex 200 (GE-Healthcare, Buckinghamshire, UK) equilibrated with the buffer, and 3-mL fractions were collected. At this step, most of the PhlG (DAPG hydrolase) was separated from the MAPG ATase. The active fractions (fractions 25–28) were pooled and placed on a column (1.2 × 12 cm) of Q Sepharose (Pharmacia, Uppsala, Sweden) equilibrated with the buffer. After it was washed with 200 mL of the buffer, the enzyme was eluted with a gradient established with 60 mL of the buffer and 60 mL of the buffer containing 1 M NaCl, and 3-mL fractions were collected. The active fractions (12–14) were pooled. The other half of the solution was treated similarly and the pooled solutions were combined. The solution was diluted with the buffer so as to make A_{280} 0.85, and was treated with $(NH_4)_2SO_4$. The precipitate obtained at 45–65% saturation was dissolved in 2 mL of the buffer and placed on a column (1.7 × 25 cm) of Superdex 200 equilibrated with the buffer, and 0.55-mL fractions were collected. The active fractions (28–34) were pooled, diluted 5-fold with H_2O, and placed on a column (1.7 × 25 cm) of hydroxyapatite (Bio-Rad, Hercules, CA) equilibrated with 10 mM potassium phosphate (pH 7.0). After it was washed with 15 mL of 10 mM potassium phosphate (pH 7.0), the enzyme was eluted with a linear gradient established with 60 mL of 10 mM potassium phosphate (pH 7.0) and 60 mL of 500 mM potassium phosphate (pH 7.0), and 3-mL fractions were collected. The active fractions (28–31) were pooled and stored on ice but not frozen, since freezing and thawing would spoil the enzyme significantly.

Enzyme assay. In 50 mM potassium phosphate (pH 7.0), DAPG showed an absorption peak at 370 nm, while MAPG and PG scarcely showed any absorption at this wavelength. Hence the enzyme activity was determined by measuring the increase (forward reaction) and the decrease (reverse reaction) in A_{370} ($\varepsilon_{370} = 6.0\,mM^{-1}\,cm^{-1}$) with a spectrophotometer UV-300 (Shimadzu, Kyoto, Japan). When the activity was measured at a different pH, the molar extinction coefficient determined at that pH was used. The reaction was carried out at 25 °C in a cuvette (light path, 1 cm). The standard reaction mixture (3 mL) contained 150 μmol of potassium phosphate (pH 7.0), 1.2 μmol of MAPG dissolved in 30 μL of ethanol, and the enzyme. The activity of the reverse reaction was determined with a mixture (3 mL) containing 150 μmol of potassium phosphate (pH 7.0), 0.3 μmol of DAPG dissolved in 30 μL of ethanol, 6 μmol of PG, and the enzyme. Unless otherwise noted, the enzyme activity was determined in the forward reaction. One unit of enzyme activity was defined as the amount catalyzing the formation or the disappearance of 1 μmol of DAPG per min under the assay conditions. Specific activity was expressed as units per mg of protein. Protein was measured by the method of Lowry *et al.*, with bovine serum albumin as standard.[23]

Identification and quantification of reaction products. After the enzyme reaction, the enzyme protein was removed by centrifugal filtration with an Amicon Ultra 10K (Millipore, Carrigtwohill, Ireland). The filtrate was applied to TLC with a silica gel 60 F_{254} (Merck, Darmstadt, Germany), and $CHCl_3$–MeOH (4:1, v/v) was used as solvent. The spots of the products detected by UV were extracted with H_2O (for PG) and with ethanol (for MAPG and DAPG). The extracts were applied again to silica gel TLC with authentic samples: the R_f-values were 0.47, 0.67, and 0.82 for PG, MAPG, and DAPG respectively.

For quantitative determination of MAPG and DAPG, the reaction mixture (0.7 mL) at equilibrium was extracted 3 times with 0.7 mL of $CHCl_3$. The extract was evaporated at 25 °C. The resulting residue was dissolved in 200 μL of 50% methanol-H_3PO_4 (pH 3.0), and 10 μL of it was analyzed by HPLC. To determine PG, the reaction mixture was deproteinized by centrifugal filtration, and the filtrate (2.5 μL) was analyzed by HPLC. HPLC was performed at 45 °C with a LC-9A HPLC system (Shimadzu) composed of a Shim-pack C_{18} reversed-phase column (0.6 × 15 cm), a LC-9A pump, a SPD-6AV UV-Vis monitor, and a C-R6A data processor. Elution was done with 50%-MeOH–H_3PO_4 (pH 3.0) at a flow rate of 0.7 mL/min. A_{310} (for MAPG and DAPG) and A_{210} (for PG) were monitored. Under these conditions, the elution times were 4.7, 7.8, and 47 min for PG, MAPG, and DAPG respectively.

Analytical methods. Polyacrylamide gel electrophoresis (PAGE) was performed with 5–15% Ready Gels J (Bio-Rad) and Davis's electrophoresis buffer.[24] SDS–PAGE was done with 12.5% polyacrylamide gel, as described by Laemmli.[25] Protein bands were stained with Coomassie Brilliant Blue R-250. Densitometric measurement of protein on the polyacrylamide gel was done with a Flying Spot Scanner (Shimadzu). Electroblotting of protein from polyacrylamide gel to polyvinylidene difluoride membrane was performed with semi-dry blotting apparatus HorizBLOT AE-6675 (Atto, Tokyo), and the N-terminal amino acid sequence was determined by Edman degradation with a Procise 492 protein sequencing system (PE Applied Biosystems, Foster City, CA). The molecular mass of the enzyme was estimated by gel filtration with Superdex 200 (1.8 × 22 cm) previously equilibrated

Table 1. Primers for PCR Cloning of *phl* Genes

Primer	Sequence[a]	Target genes
5A	5′-TGCGGATCCGCGACCCAGTTTTCTGA-3′	*phlA*, *phlAC*, *phlACB*, *phlACBD*
5C	5′-CCAGGATCCACGAGTTCAAGTACCTG-3′	*phlC*
5B	5′-CGCGGATCCGCGTGTCGCAGAACCTT-3′	*phlB*
5D	5′-TCGGGATCCCTTAACTTGTTGGCT-3′	*phlD*
3A	5′-CGGGGTACCTTGCGTAGACAGGCGTA-3′	*phlA*
3C	5′-CGGGGTACCCTGGGTACATGGACATG-3′	*phlC*, *phlAC*
3B	5′-ATGGGTACCTTCAAGGTGCCTGATAT-3′	*phlB*, *phlACB*
3D	5′-CGGGGTACCCCGGCAACGTCAGGT-3′	*phlD*, *phlACBD*

[a] *Bam*HI and *Kpn*I sites are underlined.

with 50 mM potassium phosphate (pH 7.0) and calibrated with ferritin ($M_r = 450$ kDa), bovine liver catalase (230 kDa), yeast alcohol dehydrogenase (150 kDa), bovine serum albumin (67 kDa), ovalbumin (45 kDa), and chymotrypsin (23.5 kDa).

DNA preparation and manipulation. The genomic DNA of *Pseudomonas* sp. YGJ3 was prepared by the method of Smith,[26] except that the lysate of the bacterial cells was treated at 37 °C for 30 min with protease K (1 mg/mL). A plasmid vector, pUC18, and a cosmid vector, Charomid 9-28, were obtained from Takara (Ohtsu, Japan) and Nippon Gene (Tokyo) respectively.[27,28] Oligonucleotides for sequencing primers and PCR primers and a hybridization probe were obtained from Rikaken (Nagoya, Japan). On the basis of the N-terminal amino acid sequence of a 38 kDa subunit of the purified MAPG ATase and nucleotide sequence of *phlA* of *P. fluorescens* Pf-5 (GenBank accession no. CP000076, locus tag PFL_5954), an oligonucleotide ONP1 (5′-TATGGCGCGGGTATTCCGGTATGCCGCCTG-AAA-3′) was designed. ONP1 was labeled at the 3′-terminal with digoxigenin (DIG) using a DIG-tailing label kit (Boehringer Mannheim, Mannheim, Germany), and used as probe for hybridization. Southern and colony hybridizations were performed at 56 °C. A hybridization signal on a nylon membrane was detected with a DIG luminescent detection kit (Boehringer Mannheim). All the enzymes used in DNA manipulation were purchased from Takara. Plasmid isolation and extraction of DNA from the agarose gel were done with a QIAprep kit (Qiagen, Hilden, Germany) and Suprec™-01 (Takara) respectively. DNA digestion, ligation, and transformation were done as described by Sambrook *et al.*[29]

DNA sequencing. Deletion mutants for DNA sequencing were prepared with a Kilo-sequence deletion kit (Takara) after digestion using appropriate restriction enzymes. Both strands were sequenced on denatured double-stranded DNA templates with a BigDye terminator cycle sequencing kit (Applied Biosystems, Foster City, CA) and an appropriate oligonucleotide primer (25mer). The nucleotide sequence was determined with an ABI 3100 DNA sequencer (Perkin-Elmer, Norwalk, CT). The nucleotide sequence reported in this paper has been submitted to DDBJ/EMBL/GenBank Nucleotide Sequence Databases under accession no. AB636682.

Computational tools. The nucleotide sequence and the deduced amino acid sequence were analyzed using the DNASIS program (Hitachi Software Engineering, Yokohama, Japan). Alignment was done using ClustalW (http://www.ddbj.nig.ac.jp/). The domain was located with the Pfam domain data base (http://pfam.sanger.ac.uk/), and hydrophobicity was judged with the Sosui WWW server (http://bp.nuap.nagoya-u.ac.jp/sosui/sosui_submit.html).

Cloning of the phl *gene cluster.* The genomic DNA of strain YGJ3 was digested with *Kpn*I. Southern hybridization of the *Kpn*I-digest with a DIG-labeled oligonucleotide probe ONP1 gave a single hybridization signal on a 20-kb DNA fragment. The fragment was extracted from the agarose gel and ligated into *Kpn*I-digested Charomid 9-28. After *in vitro* packaging with packaging extract Lambda inn (Nippon Gene), followed by infection of *E. coli* XL1-Blue MRA, colony hybridization gave hybridization-positive colonies. The plasmid DNA, designated pCKK20, was isolated from one of these following the handling manual of Charomid vector, and digested with *Sph*I. Agarose gel electrophoresis showed at least seven DNA fragments, at 6.3, 5.2, 3.9, 3.5, 2.8, 1.6, and 1.3 kb. Among these, the 6.3-kb fragment showed a hybridization signal. The 6.3, 5.2, and 1.3-kb fragments were introduced into *Sph*I-digested pUC18 to give plasmids pUSS6.3, pUSS5.2, and pUSS1.3 (Fig. 7). Partial DNA sequences were briefly determined by cycle sequencing with M13 forward and reverse primers (Takara). A comparison of the sequence data with those for *P. fluorescens* Pf-5 suggested that these three plasmids completely covered the *phl* gene cluster. The full DNA sequences of the three DNA fragments were determined, and were put together to complete the whole sequence (12,598-bp long) containing a *phl* gene cluster.

PCR cloning of phl *genes.* PCR amplification was carried out using PrimSTAR GXL DNA polymerase (Takara) following the protocol recommended by the manufacturer. Forward and reverse primers were designed to amplify the entire open reading frames (ORFs) including their ribosome binding sequences (Table 1). *Bam*HI and *Kpn*I sites were built into the primers for subcloning. pCKK20 was used as template DNA. The following primers flanking the target *phl* genes were used: 5A and 3A for the cloning of *phlA*; 5C and 3C for *phlC*; 5B and 3B for *phlB*; 5D and 3D for *phlD*; 5A and 3C for *phlAC*; 5A and 3B for *phlACB*; and 5A and 3D for *phlACBD* (Fig. 7). After digestion with *Kpn*I and *Bam*HI, the amplified products were ligated into *Bam*HI/*Kpn*I-digested pUC19 and transferred into *E. coli* XL1-Blue MRF′.

Gene expression in E. coli. A recombinant *E. coli* strain carrying the plasmid with *phl* genes was cultured at 37 °C in 100 mL of a LB medium containing 50 μg/mL of ampicillin. When A_{660} reached about 0.15, 1 mM isopropyl β-thiogalactopyranoside (IPTG) was added, and culturing was continued for a further 9 h. Bacterial cells were collected by centrifugation at 4 °C, washed once with 50 mM potassium phosphate (pH 7.0), and resuspended in about 6 mL of the same buffer. The cells were disrupted at 4 °C by sonication. Cell debris was removed by centrifugation at 30,000 × *g* for 15 min at 4 °C, and the supernatant (crude extract) was stored on ice to measure MAPG ATase activity.

Results

Purification of MAPG ATase

MAPG ATase was purified from a crude extract of *Pseudomonas* sp. YGJ3 grown aerobically in the absence of Cl^-. Table 2 summarizes the purification procedures, showing a 44-fold purification with a yield of about 14%. The purified enzyme preparation showed a single protein band on polyacrylamide gel electrophoresis (Fig. 2A). The protein band of MAPG ATase was observable even in the crude extract, suggesting that a significant amount of the enzyme protein was synthesized in the bacterial cells grown without Cl^-. The addition of 2 mM Cl^- or 50 μM pyoluteorin to the culture medium strongly repressed the expression of the enzyme as judged by decreased enzyme activity and decreased protein band on PAGE, while Br^- (2 mM) or I^- (2 mM) was not effective (Fig. 2B).

Table 2. Purification of MAPG ATase

Step	Protein (mg)	Sp. activity (mU/mg)	Activity (U)	Purification (-fold)	Yield (%)
Crude extract	1,260	7.33	9.24	1	100
$(NH_4)_2SO_4$ (I)	520	13.3	6.92	1.8	75
Superdex 200 (I)	136	36.4	4.95	5.0	54
Q Sepharose	35.1	97.3	3.42	13	37
$(NH_4)_2SO_4$ (II)	24.0	106	2.54	14	27
Superdex 200 (II)	15.2	122	1.85	17	20
Hydroxyapatite	4.0	323	1.29	44	14

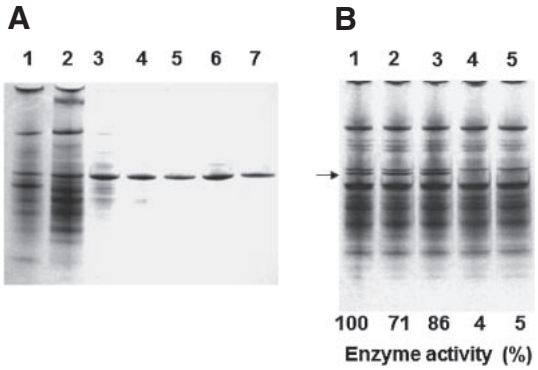

Fig. 2. Polyacrylamide Gel Electrophoresis of MAPG ATase.

A, Purification of MAPG ATase. Lane 1, crude extract (35 μg of protein); lane 2, first ammonium sulfate (31 μg); lane 3, Superdex 200 (14 μg); lane 4, Q Sepharose (10 μg); lane 5, second ammonium sulfate (1.6 μg); lane 6, hydroxyapatite (2.5 μg); lane 7, hydroxyapatite (1.3 μg). B, Effects of halide ions and pyoluteorin on the expression of MAPG ATase. *Pseudomonas* sp. YGJ3 was grown aerobically in the absence of halaid ion (lane 1), or in the presence of 2 mM I^- (lane 2), 2 mM Br^- (lane 3), 2 mM Cl^- (lane 4), or 50 μM pyoluteorin (lane 5). The crude extracts (50 μg protein), prepared as described under "Materials and Methods," except that the cell debris was removed by brief centrifugation at 10,000 *g* for 10 min, were analyzed. The relative enzyme activity of the crude extract is shown at the bottom of the lane. Arrow shows the position of MAPG ATase.

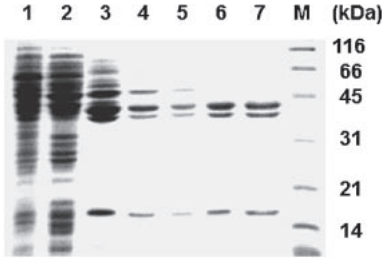

Fig. 3. SDS–PAGE of the Purification of MAPG ATase.

The samples described in the legend to Fig. 2A were applied in lanes 1–7. Lane M, marker proteins.

```
43 kDa Protein
  YGJ3   PhlC: MCARRVAIVSAAYTPKPGSSRV
  Pf-5   PhlC: MCARRVAIVSAAYTPKPGSSRV
  Q2-87  PhlC: MSARRVAIVSAAYTPKSGSSRV
               * ************** *****

38 kDa Protein
  YGJ3   PhlA: MNVKKIGIVSYGAGIPVCRLKV
  Pf-5   PhlA: MNVKKIGIVSYGAGIPVCRLKV
  Q2-87  PhlA: MN--KVGIVSYGAGIPVCRLKV
               **  * ****************

17 kDa Protein
  YGJ3   PhlB: MSMYPEQIHRMTTASMLREWRE
  Pf-5   PhlB: MSMYPEQIHRMTTASMLREWRE
  Q2-87  PhlB: MSLYPEQIHRMTTASMLREWRE
               ** ******************
```

Fig. 4. Identification of the Subunits of MAPG ATase Based on N-Terminal Amino Acid Sequences.

The N-terminal amino acid sequences of the subunits of MAPG ATase were compared with those of PhlA, PhlB, and PhlC as deduced from the nucleotide sequences of *Pseudomonas* sp. YGJ3 (GenBank accession no. AB636682), *P. fluorescens* Pf-5 (GenBank accession no. CP000076, locus tag PFL_5954-5656), and *P. fluorescens* Q2-87 (GenBank accession no. PFU41818). The sequences, determined by Edman degradation of the purified MAPG ATase, are indicated by bars above the amino acid sequences. Identical amino acid residues are shown by stars.

Molecular properties of MAPG ATase

The molecular mass of the enzyme was estimated to be about 330 ± 30 kDa by gel filtration with Superdex 200 (data not shown). On SDS–PAGE, the purified enzyme showed three protein bands at 17, 38, and 43 kDa (Fig. 3). The N-terminal amino acid sequences of these protein bands were determined by Edman degradation, and were compared with those of PhlA, PhlB, and PhlC of *P. fluorescens* (Fig. 4). The amino acid sequences of the 17, 38, and 43 kDa proteins matched PhlB, PhlA, and PhlC respectively of *P. fluorescens* Pf-5 and *P. fluorescens* Q2-87. As described below, the *phl* gene cluster of *Pseudomonas* sp. YGJ3 was cloned and sequenced. The N-terminal amino acid sequences as determined by Edman degradation were consistent with those deduced from the nucleotide sequences of strain YGJ3, except that no N-terminal residues or Cys residues were observed. These results suggest that MAPG ATase is composed of PhlA, PhlC, and PhlB. The PhlA, PhlC, and PhlB proteins obtained from triple independent experiments were measured densitometrically, and the molar ratio PhlA:PhlC:PhlB was calculated to be 0.8 ± 0.1:1.0 ± 0.1:1.2 ± 0.3 based on the M_r of these proteins. Thus MAPG ATase appears to be composed of equimolar amounts of PhlA, PhlC, and PhlB, and its subunit structure might be $(PhlACB)_3$. The purified enzyme showed an absorption maximum at 279 nm. The A_{279} of a 0.1% solution was estimated to be 0.65, and the ε_{279} was calculated to be $2.1 \times 10^5\ M^{-1}\,cm^{-1}$. The shoulder at 290 nm due to the Trp residue was not significant. The A_{280}/A_{260} ratio was 2.0. No significant absorption was detected in the visible region.

Catalytic properties of MAPG ATase

Analysis of the reaction products by the silica gel TLC and the HPLC on a C_{18} reversed-phase column indicated that the enzyme yielded DAPG and PG from

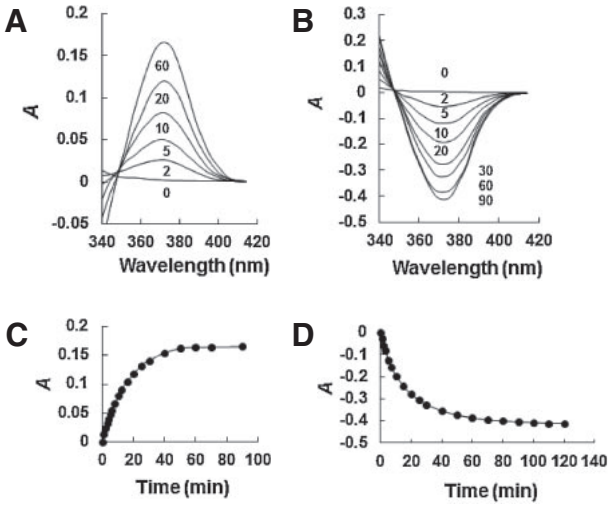

Fig. 5. Spectral Changes in MAPG ATase Reactions.
In A (forward reaction), the enzyme (95 μg) was incubated with 0.1 mM MAPG. In B (reverse reaction), it (32 μg) was incubated with 0.1 mM DAPG and 2 mM PG. All other conditions are described under "Materials and Methods." Curves were taken at the indicated times (min). C and D show the time courses of A_{370} in A and B respectively.

MAPG in the forward reaction. Similarly, MAPG was formed from DAPG plus PG in the reverse reaction. When the enzyme reaction was monitored spectrophotometrically, the absorption around 370 nm due to DAPG gradually increased in the forward reaction and decreased in the reverse reaction (Fig. 5). These results show that MAPG ATase catalyzes the disproportionation of 2 moles of MAPG to DAPG and PG. The forward and reverse reactions ceased before depletion of the substrates, indicating the establishment of equilibrium. The concentrations of MAPG, DAPG, and PG at equilibrium were measured by HPLC (Table 3). The equilibrium constant K (=[DAPG][PG]/[MAPG]^2) in the forward reaction at 25 °C with various concentrations (0.05–0.6 mM) of MAPG was estimated to be about 1.0. The K value (0.93–1.27) for the equilibrium established in the reverse reaction with various concentrations of DAPG and PG appeared to be consistent with this. DAPG was the donor of an acetyl group, but not an acceptor, since no decrease in DAPG was observed in incubation with the enzyme. Resorcinol, but not pyrocatechol, served as acetyl acceptor in place of PG in the reverse reaction.

At a fixed concentration (0.4 mM) of MAPG, activity was proportional to the amount of the enzyme added (0.024–0.19 mg). At a fixed amount of the enzyme (0.14 mg), activity increased against the MAPG concentration (0.1–1.2 mM) according to Michaelis-Menten kinetics. The K_m for MAPG and the V_{max} were estimated to be 0.26 ± 0.01 mM and 0.66 ± 0.01 μmol/min/mg respectively by double reciprocal plot. The k_{cat} was calculated to be about 1.2 s^{-1}, assuming that the enzyme (M_r = 330 kDa) has three equivalent catalytic sites. In the reverse reaction at various concentrations (0.005 mM–0.10 mM) of DAPG and at a fixed concentration (2 mM) of PG, the apparent K_m (K_m^{app}) for DAPG and the apparent V_{max} (V_{max}^{app}) were estimated to be 0.019 ± 0.001 mM and 1.55 ± 0.12 μmol/min/mg respectively. Similarly, the K_m^{app} for PG and the V_{max}^{app} were determined to be 1.31 ± 0.30 mM and 2.27 ± 0.45 μmol/min/mg respectively at various concentrations (0.2–3 mM) of PG and at a fixed concentration (0.1 mM) of DAPG. Resorcinol was an active acetyl acceptor. The K_m^{app} and a V_{max}^{app} were estimated to be 0.77 ± 0.06 mM and 0.81 ± 0.08 μmol/min/mg respectively. DAPG inhibited the forward reaction competitively ($K_i = 0.018 \pm 0.001$ mM), while PG showed no significant inhibition ($K_i \geq 13$ mM). Acetyl-CoA (1 mM) and malonyl-CoA (1 mM) had no significant effects on enzyme activity. The kinetic mechanism of the MAPG ATase reaction could not be determined, because an accurate assay in the reverse reaction with a low concentration of DAPG was difficult.

Table 3. Estimation of the K Value of the MAPG ATase Reaction

Substrate (conc. (mM))	Conc. at equilibrium (mM)			K[a]
	MAPG	DAPG	PG	
MAPG (0.05)	0.0132	0.0169	0.0091	0.88
MAPG (0.1)	0.0249	0.0283	0.0208	0.95
MAPG (0.2)	0.0576	0.0593	0.0564	1.01
MAPG (0.4)	0.107	0.114	0.118	1.17
MAPG (0.6)	0.177	0.186	0.172	1.02
DAPG (0.0333) + PG (2)	0.0466	0.004	1.97	1.27
DAPG (0.1) + PG (2)	0.168	0.0161	1.97	1.12
DAPG (0.1) + PG (0.2)	0.0996	0.0579	0.160	0.93

[a] K = [DAPG][PG]/[MAPG]^2

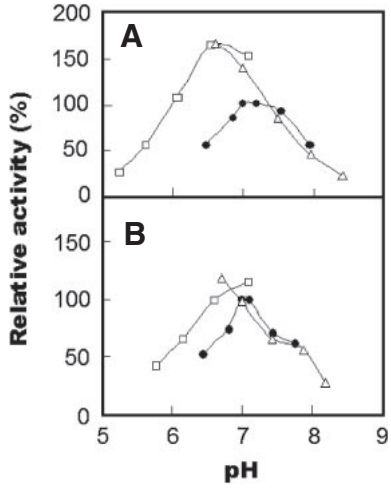

Fig. 6. pH Dependence of MAPG ATase.
The forward (A) and the reverse (B) reactions were measured in the following buffers (each 50 mM): 2-morpholinoethanesulfonic acid (MES) (□); potassium phosphate (●); HEPES (△). The activity obtained with potassium phosphate, pH 7.0, was taken to be 100%.

Effects of temperature, pH, and inhibitors on MAPG ATase

When the enzyme activity was measured at various temperatures, it increased as the temperature increased up to 65 °C (data not shown). The enzyme was preincubated in 50 mM potassium phosphate (pH 7.0) for 20 min at various temperatures and then residual activity was measured. The enzyme retained activity below 40 °C, but was inactivated at above 65 °C, suggesting that it was moderately thermostable.

The forward and the reverse reactions showed optimum pH at about 6.3–7.2 (Fig. 6). The highest activity was obtained with 2-morpholinoethanesulfonic

Table 4. Genes Involved in DAPG Biosynthesis

Gene	Location of DNA sequence	No. of amino acid residues	Deduced M_r (kDa)	Function
phlH	2,259–2,930, C[a]	223	24.2	Regulatory protein[14]
phlG	3,072–3,956	294	33.7	DAPG hydrolase[14,15]
phlF	4,008–4,610, C	200	22.9	Regulatory protein[12]
phlA	5,072–6,160	362	38.5	MAPG ATase 39 kDa subunit[11]
phlC	6,190–7,386	398	42.5	MAPG ATase 43 kDa subunit[11]
phlB	7,399–7,839	146	16.6	MAPG ATase 17 kDa subunit[11]
phlD	8,048–9,097	349	38.6	Polyketide synthase[11,19,20]
phlE	9,207–10,472	421	44.9	Permease[11,13]
phlI	10,479–11,411	310	35.3	Putative uncharacterized protein[7]

[a]Complement

acid (MES) and HEPES buffers. These buffers showed some absorption at 210 nm, and interfered with the measurement of PG by HPLC. Hence potassium phosphate buffer was used throughout this study.

To examine the effects of various reagents on MAPG ATase activity, the enzyme was preincubated with various reagents at 25 °C for 5 min and then residual activity was measured. $HgCl_2$ (0.1 mM) and *p*-chloromercuribenzoate (1 mM) completely inactivated the enzyme. It lost 88% of its activity after it was treated with diethylpyrocarbonate (1 mM). Various metal compounds (1 mM each), including NaCl, $MgCl_2$, $CaCl_2$, $FeCl_3$, $ZnCl_2$, $CuCl_2$, and $NiCl_2$, and various metal chelators (0.5 mM each), including 1,10-phenanthroline, 8-hydroxyquinoline, 2,2′-dipyridine, and tiron (catechol-3,5-disulfonic acid disodium salt), had almost no effect on enzyme activity. Neither activation nor inhibition was found with thiols (1 mM each) such as L-cysteine, 2-mercaptoethanol, and dithiothreitol.

Cloning and expression of phl *genes*

A *Kpn*I 20-kb DNA fragment was cloned with Charomid 9-28 from genomic DNA of *Psedomonas* sp. YGJ3, as described above under "Materials and Methods." The resulting plasmid, pCKK20, was digested with *Sph*I. Of the DNA fragments formed, 6.3, 5.2, and 1.3-kb DNA fragments were subcloned into pUC18 for DNA sequencing. Finally, the sequence of a 12,598-bp long DNA region was determined to define the organization of DAPG biosynthetic locus *phlHGFACBDEI* (Fig. 7). Table 4 summarizes the features of these genes. A possible promoter sequence (TTAAGA for the −35 sequence and TATTAC for the −10 sequence) was present in the region upstream of *phlA* (nucleotide numbers 4,825–4,854). Although no ρ-independent terminator sequence was found, another terminator must have been present in the region downstream of *phlI*. The deduced amino acid sequences of all the *phl* genes agreed almost completely with those of *P. fluorescens* Pf-5 (more than 99% identities), but were less homologous (80–93% identities) to those of *P. fluorescens* Q2-87. PhlA had a 3-oxoacyl-acylcarrier protein synthase (ACP synthase) III domain, as described by Bangera and Thomashow,[11] although the overall sequence homology between *Pseudomonas* sp. YGJ3 PhlA and *E. coli* K12/DH10B ACP synthase III (UniProt accession no. B1XA01) was low (19% identical). PhlA lacked the active site Cys and His residues, which are well conserved in ACP synthase III of various species.[30]

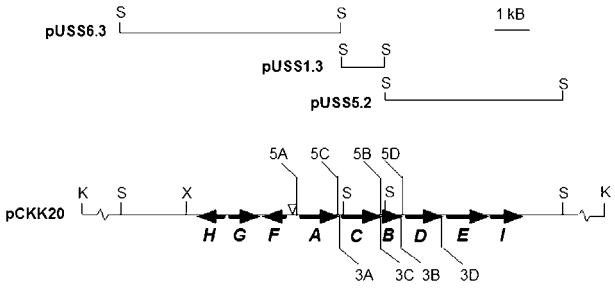

Fig. 7. Organization of the *phl* Gene Cluster from *Pseudomonas* sp. YGJ3.

The above horizontal lines show the insert DNA of plasmids pUSS6.3, pUSS1.3, and pUSS5.2, which were used in sequencing a 12,598-bp long DNA region containing the *phl* gene cluster. *phl* gene cluster *phlHGFACBDEI* is shown by bold arrows on the below horizontal line, which shows a *Kpn*I 20-kb DNA fragment cloned into Charomid 9-28. ORFs indifferent as to *phl* genes are not shown. The hybridization sites of forward primers (5A–5D) and reverse primers (3A–3D) for PCR cloning are shown. The solid triangle shows the position of a possible promoter. Several restriction sites are marked: K, *Kpn*I; S, *Sph*I; X, *Xba*I.

PhlC had a thiolase-like domain, including active site His and Cys residues,[31] although the overall sequence homology between PhlC and *E. coli* K12/DH10B 3-ketoacyl-CoA thiolase (UniProt accession no. B1X9L5) was low (16% identity). PhlB of *Pseudomonas* sp. YGJ3 had a Cys-rich region: there were 5 Cys residues in the region of residue no. 34–61). It had no known enzyme domain, but a DUF (domain of unknown function) 35 OB-fold domain, which is frequently found in DNA binding proteins.[32] Analysis of hydrophobicity indicated that PhlA, PhlC, PhlB, PhlD, PhlF, PhlG, PhlH, and PhlI are soluble proteins, while PhlE is a membrane protein.[11]

To express *phl* genes in *E. coli*, PCR cloning with pCKK20 as template was performed using appropriate forward and reverse primers (Table 1 and Fig. 7). The PCR products were digested with *Bam*HI and *Kpn*I and introduced into pUC19 to construct plasmids pU*phlA*, pU*phlB*, pU*phlC*, pU*phlD*, pU*phlAC*, pU*phlACB*, and pU*phlACBD*. The nucleotide sequences of the DNA inserts of these plasmids were confirmed by cycle sequencing with appropriate sequencing primers. Expression of the *phl* genes in *E. coli* XL1-Blue MRF′ was induced by the addition of 1 mM IPTG in a culture medium. When the culture broth of the recombinant *E. coli* was extracted with $CHCl_3$ and analyzed by HPLC, neither MAPG nor DAPG was detected. However, significant activity of MAPG ATase was found in

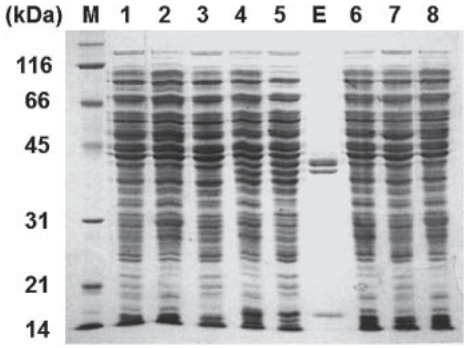

Fig. 8. Expression of *phl* Genes in *E. coli*.

SDS–PAGE was done with a large gel ($13.8 \times 10 \times 0.1$ cm) to analyze crude extracts (50 μg protein) of the following recombinant *E. coli*: *E. coli* XL1-Blue MRF′ carrying pUC19 (lane 1), pU*phlA* (lane 2), pU*phlAC* (lane 3), pU*phlACB* (lane 4), pU*phlACBD* (lane 5), pU*phlB* (lane 6), pU*phlC* (lane 7), or pU*phlD* (lane 8). Lane M, marker proteins; lane E, MAPG ATase (about 1 μg) purified from *Pseudomonas* sp. YGJ3.

crude extracts from *E. coli* XL1-Blue MRF′ harboring pU*phlACB* (specific activity, 7.6 ± 0.4 mU/mg) and pU*phlACBD* (16.6 ± 1.1 mU/mg). The product of the enzyme reaction was extracted, and was confirmed to be DAPG by HPLC. No other recombinant *E. coli* showed MAPG ATase activity. SDS–PAGE of the crude extract from *E. coli* carrying pU*phlA*, pU*phlC*, pU*phlB*, pU*phlD*, or pU*phlAC* showed faint bands of the corresponding gene products. The crude extract from *E. coli* carrying pU*phlACB* or pU*phlACBD* gave protein bands characteristic of MAPG ATase, although the bands of PhlC and PhlB were somewhat disturbed by proteins intrinsic to *E. coli* (Fig. 8). Expression of MAPG ATase was also confirmed by native PAGE (data not shown). When crude extracts of *E. coli* harboring pU*phlA*, pU*phlC*, pU*phlB*, and pU*phlD* were mixed and incubated at 4 °C for 5 min or for 12 h in the presence and the absence of 1 mM 2-mercaptoethanol, no MAPG ATase activity was reconstructed. The crude extract of *E. coli* carrying pU*phlD* activated neither the enzyme in the crude extract of *E. coli* carrying pU*phlACB* nor the enzyme purified from *Pseudomonas* sp. YGJ3, but rather somewhat inhibited them, possibly due to PhlD-derived metabolites (data not shown).

Discussion

DAPG and MAPG show similar UV spectra at wavelengths longer than 300 nm in an organic solvent.[33] In neutral aqueous solution, DAPG but not MAPG exhibits a significant absorption peak at 370 nm. Based on this, we established a convenient spectrophotometric assay for MAPG ATase and purified it from an extract of *Pseudomonas* sp. YGJ3 to elucidate its properties. In concurrence with the findings of Bangera and Thomashow, that *phlACB* is essential for the conversion of MAPG to DAPG,[11] the MAPG ATase molecule was indeed composed of PhlA, PhlC, and PhlB (Fig. 4). PCR cloning of the *phlACB* genes followed by expression in *E. coli* further confirmed the molecular identity of PhlACB with MAPG ATase.

E. coli XL1-Blue MRF′ carrying pU*phlACBD* scarcely produced MAPG or DAPG in the culture broth in spite of high-level expression. Since recombinant *E. coli* had no significant activity hydrolyzing MAPG and DAPG (data not shown), this was partly due to a lack of PhlE (permease), but chiefly due to the low DAPG production of the recombinant *E. coli*. Achkar *et al.* showed that *P. fluorescens* Pf-5 transformed with a plasmid containing a *phlACBDE* insert produced large amounts of PG, MAPG, and DAPG, while recombinant *E. coli* carrying *phlACBDE* synthesized only a little MAPG, and scarcely produced DAPG.[19] Thus, in addition to *phlACBD*, some other factors inherent in *P. fluorescens* cells but limited in *E. coli* cells appear to be required to facilitate DAPG biosynthesis. In connection with this, it is probable that *phlI* plays a role in DAPG biosynthesis.

PhlA, PhlC, and PhlB are integral subunits of MAPG ATase (Fig. 4). PhlA and PhlC have enzyme domains related to an acetyl transfer, while the intrinsic function of PhlB in enzymatic catalysis remains uncharacterized. Since *phlACB* and *phlACBD* were expressed at higher degrees in *E. coli* than *phlA*, *phlC*, *phlB*, *phlD*, and *phlAC* (Fig. 8), *phlB* appeared to facilitate high-level gene expression. The DUF 35 OB-fold in PhlB suggests that PhlB somewhat interacts with DNA, although no direct evidence for this has been obtained. MAPG ATase activity was intricately affected by *phlD*. *phlD* increased MAPG ATase activity by coexpression with *phlACB*, while independent expression of *phlD* led to the production of the inhibitors of MAPG ATase.

MAPG ATase catalyzes the transfer of acetyl groups among DAPG, MAPG, and PG. This explains the observation that recombinant *E. coli* carrying *phlACB* produced no DAPG, MAPG, or PG, but stimulated their interconversion when they were added exogenously into the culture medium.[19] If MAPG is biosynthesized by PhlD, MAPG ATase can convert it to DAPG, but PhlD-His_6 synthesizes PG but not MAPG, as reported by Zha *et al.*[20] To synthesize MAPG and DAPG from PG, MAPG ATase must be provided with a sufficient amount of appropriate acetyl donor. Contrary to our expectations, acetyl-CoA appeared to be inactive as a donor substrate for purified MAPG ATase. Achkar *et al.* have reported that recombinant *E. coli* carrying *phlACBD* produced a small amount of MAPG under culture conditions different from those used in this study.[18] Hence there must be an acetyl donor in *E. coli* cells.

PG and its derivatives are found in various natural products. PG is known to be formed by enzymatic hydrolysis of phloretin,[34] enzymatic *trans*-hydroxylation between pyrogallol and 1,2,3,5-trihydroxybenzene,[35] and PhlD-catalyzed Claisen condensation of malonyl-CoA.[19,20] The MAPG ATase reaction described in this study is a new biological source of PG.

In conclusion, we purified and characterized *Pseudomonas* sp. YGJ3 MAPG ATase for the first time. We also cloned *phl* genes to confirm that *phlACB* is necessary and sufficient for the synthesis of MAPG ATase. In contrast to most acetyl transferases using CoA derivatives as acyl donors or acceptors, MAPG ATase catalyzes the transfer of acetyl groups without intermediation of CoA derivatives. It is an interesting problem how this rare transferase catalyzes the cleavage and formation of C–C bonds. It is probable that *in vivo* MAPG ATase interacts with PhlD facilitating the efficient transfer of intermediates between these functionally related enzymes.

The present study should prove useful in future investigation of the interaction between MAPG ATase and PhlD and of the structure and catalytic mechanism of MAPG ATase.

References

1) Leisinger T and Margraff R, *Microbiol. Rev.*, **43**, 422–442 (1979).
2) van Pée K-H and Ligon JM, *Nat. Prod. Rep.*, **17**, 157–164 (2000).
3) Dowling DN and O'Gara F, *Trends Biotechnol.*, **12**, 133–141 (1994).
4) Loper JE, Kobayashi DY, and Paulsen IT, *Phytopathology*, **97**, 233–238 (2007).
5) Nowak-Thompson B, Gould SJ, Kraus J, and Loper JE, *Can. J. Microbiol.*, **40**, 1064–1066 (1994).
6) Keel C, Weller DM, Natsch A, Défago G, Cook RJ, and Thomashow LS, *Appl. Environ. Microbiol.*, **62**, 552–563 (1996).
7) Moynihan JA, Morrissey JP, Coppoolse ER, Stiekema WJ, O'Gara F, and Boyd EF, *Appl. Environ. Microbiol.*, **75**, 2122–2131 (2009).
8) Keel C, Schnider U, Maurhofer M, Voisard C, Laville J, Burger U, Wirthner P, Haas D, and Défago G, *Mol. Plant Microbe Interact.*, **5**, 4–13 (1992).
9) Laville J, Voisard C, Keel C, Maurhofer M, Défago G, and Haas D, *Proc. Natl. Acad. Sci. USA*, **89**, 1562–1566 (1992).
10) Fenton AM, Stephens PM, Crowley J, O'Callaghan M, and O'Gara F, *Appl. Environ. Microbiol.*, **58**, 3873–3878 (1992).
11) Bangera MG and Thomashow LS, *J. Bacteriol.*, **181**, 3155–3163 (1999).
12) Delany I, Sheehan MM, Fenton A, Bardin S, Aarons S, and O'Gara F, *Microbiology*, **146**, 537–546 (2000).
13) Abbas A, McGuire JE, Crowley D, Baysse C, Dow M, and O'Gara F, *Microbiology*, **150**, 2443–2450 (2004).
14) Bottiglieri M and Keel C, *Appl. Environ. Microbiol.*, **72**, 418–427 (2006).
15) He Y-X, Huang L, Xue Y, Fei X, Teng Y-B, Rubin-Pitel SB, Zhao H, and Zhou C-Z, *J. Biol. Chem.*, **285**, 4603–4611 (2010).
16) Ferrer J-L, Jez JM, Bowman ME, Dixon RA, and Noel JP, *Nat. Struct. Biol.*, **6**, 775–784 (1999).
17) Austin MB and Noel JP, *Nat. Prod. Rep.*, **20**, 79–110 (2003).
18) Shanahan P, Glennon JD, Crowley JJ, Donnelly DF, and O'Gara F, *Anal. Chim. Acta*, **272**, 271–277 (1993).
19) Achkar J, Xian M, Zhao H, and Frost JW, *J. Am. Chem. Soc.*, **127**, 5332–5333 (2005).
20) Zha W, Rubin-Pitel SB, and Zhao H, *J. Biol. Chem.*, **281**, 32036–32047 (2006).
21) Matano I, Tsunekawa M, Shimizu S, Tanaka I, Mitsukura K, and Maruyama K, *Biosci. Biotechnol. Biochem.*, **74**, 427–429 (2010).
22) Jerpseth B, Greener A, Short JM, Viola J, and Kretz PL, *Strat. Mol. Biol.*, **5**, 81–83 (1992).
23) Lowry OH, Rosebrough NJ, Farr AL, and Randall RJ, *J. Biol. Chem.*, **193**, 265–275 (1951).
24) Davis BJ, *Ann. NY Acad. Sci.*, **121**, 404–427 (1964).
25) Laemmli UK, *Nature* (London), **227**, 680–685 (1970).
26) Smith MG, *Methods Enzymol.*, **12A**, 545–550 (1967).
27) Yanish-Perron C, Vieira J, and Messing J, *Gene*, **33**, 103–119 (1985).
28) Saito I and Stark GR, *Proc. Natl. Acad. Sci. USA*, **83**, 8664–8668 (1986).
29) Sambrook J, Fritsch EF, and Maniatis T, "Molecular Cloning, a Laboratory Manual" 2nd ed., Cold Spring Harbor Laboratory, Cold Spring Habor (1989).
30) Khandekar SS, Gentry DR, van Aller GS, Warren P, Xiang H, Silverman C, Doyle ML, Chambers PA, Konstantinidis AK, Brandt M, Daines RA, and Lonsdale JT, *J. Biol. Chem.*, **276**, 30024–30030 (2001).
31) Jiang C, Kim SY, and Suh D-Y, *Mol. Phylogenet. Evol.*, **49**, 691–701 (2008).
32) Muzin AG, *EMBO J.*, **12**, 861–867 (1993).
33) Marchand PA, Weller DM, and Bonsall RF, *J. Agric. Food Chem.*, **48**, 1882–1887 (2000).
34) Chatterjee AK and Gibbins LN, *J. Bacteriol.*, **100**, 594–600 (1969).
35) Brune A and Schink B, *J. Bacteriol.*, **172**, 1070–1076 (1990).